

# Fuzzy force learning controller of flexible wiper system

Ali Zolfagharian · P. Valipour · S. E. Ghasemi

Received: 17 July 2014 / Accepted: 22 February 2015 / Published online: 7 March 2015  
© The Natural Computing Applications Forum 2015

**Abstract** Wiper blade of automobile is among those types of flexible system that is required to be operated in quite high velocity to be efficient in high load conditions. This causes some annoying noise and deteriorated vision for occupants. The modeling and control of vibration and low-frequency noise of an automobile wiper blade using soft computing techniques are focused in this study. The flexible vibration and noise model of wiper system are estimated using artificial intelligence system identification approach. A PD-type fuzzy logic controller and a PI-type fuzzy logic controller are combined in cascade with active force control (AFC)-based iterative learning (IL). A multi-objective genetic algorithm is also used to determine the scaling factors of the inputs and outputs of the PID-FLC as well as AFC-based IL gains. The results from the proposed controller namely fuzzy force learning (FFL) are compared with those of a conventional lead–lag-type controller and the wiper bang–bang input. Designing controllers based on classical methods could become tedious, especially for systems with high-order model. In contrast, FFL controller design requires only tuning of some scaling factors in the control loop and hence is much simpler and efficient than classical design methods.

**Keywords** Automotive wiper · System identification · Intelligent control · Multi-objective genetic algorithm

## 1 Introduction

Flexibility feature of wiper blade structure has made it a critical apparatus in terms of control matter in spite of its uncomplicated operational mechanism. A desirable wiper system is characterized by a homogeneous disposal of the water, without noise generation and by limiting as much as possible the phenomenon of wear (loss of wiping or noise presence). Low-frequency noise known as chatter noise was identified in wiper system during operation and is subjected to be suppressed while does not violate other oscillatory attributions of wiper system in time domain [3]. This noise causes annoying sound to automobile occupant during the wiper operation especially in the heavy rain and snow.

Flexible dynamic of a wiper system requires a reliable system identification method to model transfer function of wiper system for helping designer in developing more accurate controller. Modeling of wiper system as a flexible manipulator with several modes needs a trustworthy system identification method featuring capability at fast-varying dynamics and non-minimum phase systems modeling [22, 28]. A nonlinear auto-regressive exogenous (NARX) [8] in cascade with Elman neural network (ENN) is utilized for the purpose of system identification of nonlinear wiper system [9, 24].

Pole placement controller was applied in vibration reduction in flexible smart structures [13]. Adaptive and robust pole placement approaches were proposed for vibration and noise reduction in cantilever beams [25, 31]. Inverse dynamics control in cooperation with input shaping

---

A. Zolfagharian  
Department of System Dynamics and Control, Universiti  
Teknologi Malaysia, Johor Bahru, Johor, Malaysia

P. Valipour  
Department of Textile and Apparel, Qaemshahr Branch,  
Islamic Azad University, Qaemshahr, Iran

S. E. Ghasemi (✉)  
Young Reseachers and Elite Club, Qaemshahr Branch,  
Islamic Azad University, Qaemshahr, Iran  
e-mail: s.ebrahim.ghasemi@gmail.com

was developed to achieve minimum vibration within bounded speed of actuator [21]. The vibration control of chaotic motion in a two-blade wiper system was investigated by Wang and Chau [27]. A hybrid control method for a flexible inverted pendulum on a moving cart deals with the vibration of system with minimum actuator effort [2]. Yanyan et al. [29] proposed a control approach by sensing the rain extent on windscreen using infrared rain sensor that commands the motor velocity proportionally. Prakash and Anita [20] employed fuzzy logic controller along with a conventional model reference adaptive control (MARC) to deal with nonlinear traits of system.

For systems subject to external disturbances, nonlinearities, uncertainties, and signal limits, obtaining a precise model of the system in various operating conditions is very difficult. Thus, model-free controllers have been recently emerged in the literature [12]. Although the model of the system is required in the controller design stage, an exact model of the system is not required for controller synthesis. PD-type fuzzy controller (PD-FLC) and PI-type fuzzy controller (PI-FLC) are the most common reported methods in the literature [19]. The advantage of using the PD-FLC is that unlike conventional controller design methods, the exact model of the system is not required at the controller design stage. PD-FLC improves the transient response of the system. However, the steady state error of the system will remain large when PD-FLC is employed. PI-FLC control is known to be more practical than PD-FLC, because it results in zero steady state error [14]. Since PI-FLC is still known to give poor performance for high-order processes due to the integral action, the three-term PID-FLC control should enhance the performance.

In order for three-term PID-FLC control to enhance the performance, it needs three inputs to the fuzzy controller, which makes the design of rule-bases very difficult ( $N_i \times N_j \times N_k$ , where  $N_i$ ,  $N_j$ , and  $N_k$  are the number of membership functions of the inputs) [7]. An alternative approach to alleviate this problem is to add an integrator to the output of the PD-FLC and sum it to the PD part. It basically produces a PD-FLC + I not a PID-FLC [15].

In order to design a PID-FLC, we combined two separate PI-FLC and PD-FLC. This structure simplifies the configuration and makes the controller easier to implement, since both rule-bases are two-dimensional. The problem then becomes designing a PI and a PD rule-base, which reduces the complexity of the design [10]. After designing the fuzzy controller, fine-tuning can be made in order to improve the performance of the controller. Tuning can be made either to the membership functions or to the scaling factors (note that it is common to use normalized inputs and outputs for fuzzy controller and hence scaling factors are required to normalize these inputs and outputs). However, as the rule-base conveys a general control policy, it is

preferred to keep the rule-base unchanged and the tuning exercise is focused on the scaling factors. In multi-objective control problem, it is necessary to estimate a number of parameters of control scheme that in turn introduces more complexity to the system. To tackle this, multi-objective genetic algorithm (MOGA) was utilized to optimize the PID-FLC scaling factors in order to achieve the optimum trade-off between the desired objective functions [18, 23]. Population-based optimization technique like bees colony was successfully applied for exploiting the most appropriate parameters of fuzzy membership function and simplified the fuzzy control design while enhances the control effectiveness [5].

Iterative learning (IL) method is an intelligent learning algorithm for mechanisms that perform repetitive operations within a period of time to improve the system's performance. In other words, IL control is a learning method to generate an optimal output response as close as the desired output as time increases. Arimoto proposed a number of learning algorithms and proved their convergence, stability, and robustness [1]. Since then, IL control has been successfully applied to different repetitive flexible control systems [4, 26, 30].

A reliable nonlinear system identification namely nonlinear auto-regressive exogenous Elman neural network (NARXENN) was adopted in first stage of this survey to model the flexible dynamics of wiper blade with acquired experimental data. A lead-lag controller was designed based on the dynamics properties of wiper system extracted from system identification and applied on the path of reference input. Then, a PD-FLC and a PI-FLC are combined in cascade with active force control (AFC)-based IL and named fuzzy force learning (FFL) to achieve a robust controller for possible uncertainty that occurs during operation of wiper. In order to deal with complexity of controlling the multi-conflict objectives in both time and frequency domains, MOGA is utilized to regulate the corresponding parameters of proposed controller. Detail of the proposed controller is illustrated in Fig. 1.

Methodology of data acquisition and design of the controllers are presented in Sect. 2. In Sect. 3, the results

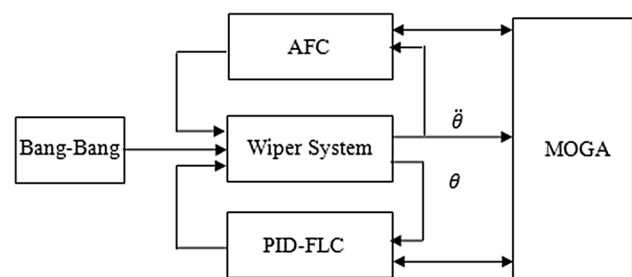


**Fig. 1** FFL controller using MOGA

of system identification and effectiveness of proposed controller are discussed, and finally, the conclusion is brought in Sect. 4.

## 2 Methodology

### 2.1 Data acquisition

First, the data acquisition stage is carried out online for recording the wiper system signals. Then, the data analyses run off-line and handle the recorded data to develop an efficient controller standing by experimental tests. A uni-blade-type wiper, which is typically found in the Proton Iswara and is driven by its corresponding DC wiper motor in hub, measuring devices, interface card, and digital processor are in hand for experiment. The wiper blade can be considered as a pinned-free flexible arm that moves freely in the horizontal plane of windscreen while the effect of axial force is negligible. A pipe hose with running water is facilitated on the top of windscreen that simulates a rainy or wet condition for operating wiper at speed of bang–bang input. The measurement sensors included a Kistler Type 8794A500 tri-axial accelerometer mounted at the endpoint of the wiper blade using beeswax for measurement of endpoint acceleration as well as a shaft encoder placed at the hub of wiper for measurement of hub angle. Recording the input signals is carried out at digital sampling rate of 1 kHz. In the experiment, a 16-input-channel PAK MK II Muller BBM signal analyzer was used.

The simulation of the flexible manipulator is conducted with the two analogue outputs namely hub angle and endpoint acceleration. Low-pass filters each with cutoff frequency of 80 Hz is used to band limit the system response to the first resonance mode for each output. Furthermore, to decouple the flexible motion control loop from the rigid body dynamics, a high-pass filter for each output

with a cutoff frequency of 5 Hz is used. The system damping ratio is negligible, and payload is measured as 7.4 N/m. A motor drive amplifier (current amplifier) delivers a current proportional to the input voltage for actuating a bidirectional motor. A linear drive amplifier LA5600 can be employed as motor driver too. The shaft encoder placed on hub of wiper sends the analogue information of the hub angle of the wiper to process unit of controller after being converted to digital values. An interface circuit PCL 812PG is needed to interface the wiper system with a host PC and carrying out data acquisition and control between the processor, the actuator, and sensors with 25 μs for A/D conversion and a settling time of 20 μs for D/A conversion. A schematic diagram of proposed controller interfaces used in this work is shown in Fig. 2.

### 2.2 AFC-based IL

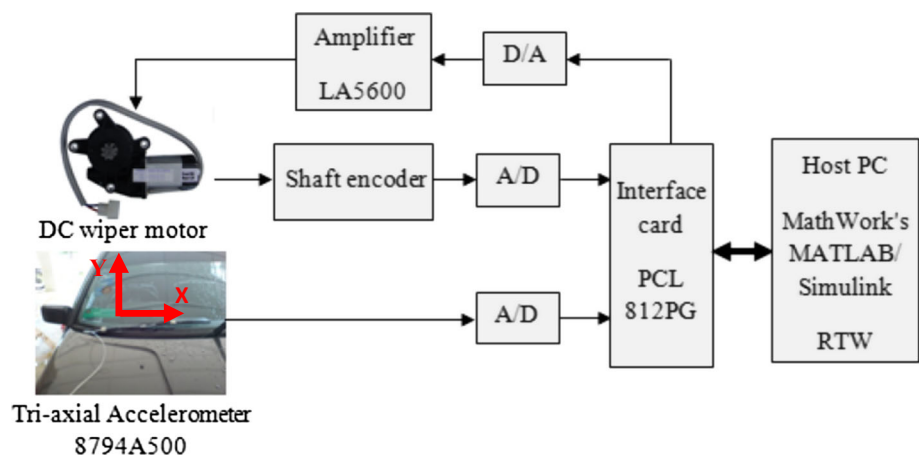
The AFC technique verified to be quite effective in robust accuracy positioning tasks in spite of possessing trouble-free mathematical algorithm [11]. The successful operation of AFC method as a disturbance rejecter scheme compared to the traditional control methods such as the PID controller is proved in the literature [16, 17, 24]. Other advantages of application of AFC as a disturbance rejection in this study are because of its low computational burden and few input information in a real time system. As it is shown in Fig. 3, AFC requires only the acceleration information of wiper tip.

In the rotational bodies, Newton’s second law expresses that the sum of all torques applied to the system is equal to the multiplication of the mass moment of (*I*) to the angular acceleration ( $\alpha$ ) of the system.

Consider Newton’s well-known and functional second law of motion of rotational bodies:

$$\sum \tau = I\alpha \tag{1}$$

**Fig. 2** Schematic diagram of proposed controller interfaces



where  $\tau$  is the applied torque of wiper motor and  $I$  and  $\alpha$  are the mass moment of inertia and the angular acceleration of the wiper blade, respectively.

An external disturbance  $\tau_d$  is included in (1):

$$\tau + \tau_d = I(\theta)\alpha \tag{2}$$

The main point of AFC is where disturbances have to be estimated somehow as:

$$\tau_d^* = \tau - EI\alpha \tag{3}$$

where **EI** is the estimated inertia matrix that can be obtained by crude approximation or other intelligent methods such as iterative learning, fuzzy logic. MOGA has been used in this paper to estimate the most appropriate value for **EI** to achieve a desirable trade-off among all objectives even in the presence of external disturbance.  $\tau$  is the measured applied control torque that can be estimated by a current sensor or directly by a force or torque sensor, and the measured angular acceleration, i.e.,  $\ddot{\theta}$  can be obtained

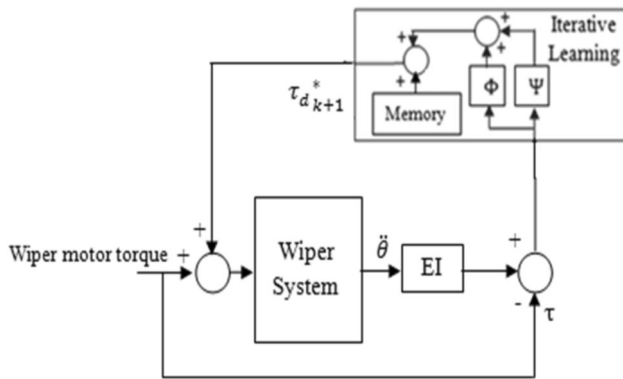


Fig. 3 AFC-based IL

by an accelerometer. From (3), it is clear that if the total applied torque to the system and angular acceleration of actuated joint are accurately obtained using measuring instruments, the estimated inertial parameters needed in AFC loop for disturbance rejection are appropriately approximated, without having to acquire the knowledge about actual magnitude of the disturbance. In order to alleviate the total torque disturbance, IL compensator is incorporated in AFC loop as well (Fig. 3).

Most of the algorithms proposed by Arimoto et al. in the literature show that the  $(k + 1)$ th input to the system can be obtained by  $k$ th input plus an error coefficient that may consist of a coefficient of track error ( $TE = q_{desired} - q_{actual}$ ), derivative and integral of track error. These mathematical expressions are similar to the description of classic PID controller; therefore, the IL algorithms can be described as the proportional-integral (PI)-type learning algorithms as follows:

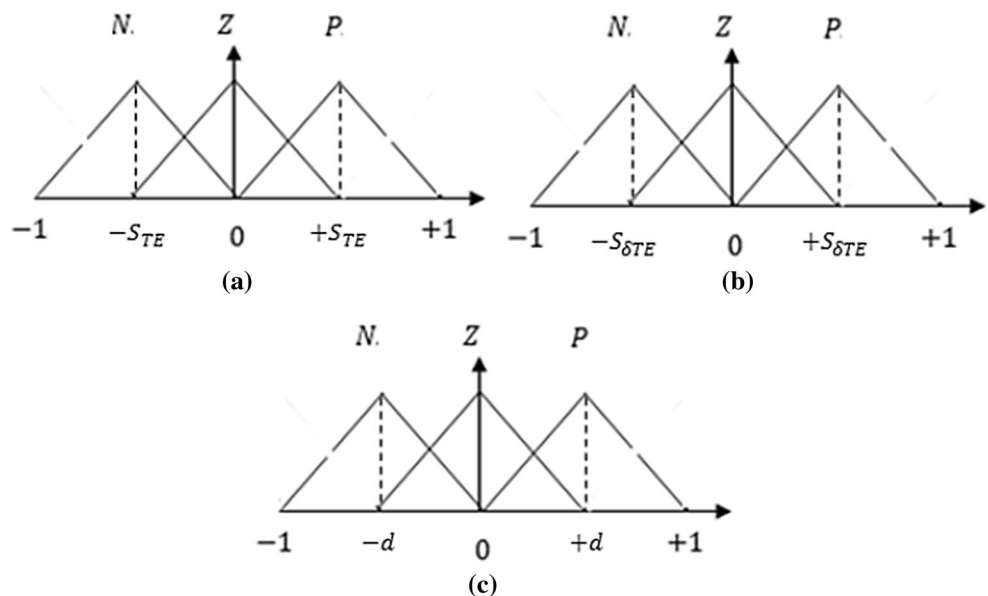
$$\tau_{d_{k+1}}^* = \tau_{d_k}^* + \left( \phi + \psi \int dt \right) e_k \tag{4}$$

where  $\tau_{d_{k+1}}^*$  and  $\tau_{d_k}^*$  are the next step and current estimated inertia for AFC loop,  $e_k$  is the output error ( $TE = q_{desired} - q_{actual}$ ),  $\phi$  and  $\psi$  are learning parameters of PI-type iterative learning algorithm. The most appropriate values of  $\phi$  and  $\psi$  are carefully obtained using crude approximation.

### 2.3 PID-FLC

In order to reduce the number of rules that are used in regular three-input PID-type fuzzy controller, two separate Sugeno-type FLC structures are used in this paper. In fact,

Fig. 4 Membership functions illustration of FLC: **a** track error input, **b** rate of track error input, **c** controller output



the PID action is separated into a PI-FLC and a PD-FLC part. The outputs from the two fuzzy controllers are then added together to result in a final PID-FLC. The inputs to both the PI-FLC and the PD-FLC parts are scaled error ( $e(t)$ ) and the scaled rate of change of error ( $\dot{e}(t)$ ). The size of inputs and output membership functions is chosen to be three. The membership functions of the input and output variables for both the PI-FLC and the PD-FLC to be employed are of the triangular type, and they are defined as shown in Fig. 4 and Table 1. Since both the PD-FLC and

PI-FLC parts share the same inputs, the number of rules has been reduced to  $3 \times 3 + 3 \times 3$  instead of regular three-input PID-FLC controller with  $(3 \times 3 \times 3)$  rules. Note that the universe of discourse for both the PI-FLC and the PD-FLC is normalized between  $[-1, 1]$ . Thus, three scaling factors namely  $S_{TE}$ ,  $S_{\delta TE}$ , and  $S_u$  (Fig. 5) are required to be designed and tuned using MOGA in the following section.

### 2.4 MOGA

In MOGA, fitness sharing technique is utilized to give confidence in the search toward the true Pareto optimal set while maintaining diversity in the population. The basic idea of fitness sharing is that all the individuals within the same region (called a niche) share their fitness. In fitness sharing method, a niche count is obtained from the Euclidean distance between every pair of solutions first and then the fitness of each solution is ranked from the best individual to the worst. Details of this method can be found in Ref. [6]. Also, hypervolume indicator is adopted in this study for performance assessment of MOGA [32].

**Table 1** FLC rule-base with track error and rate of track error

Track error (TE)	Rate of track error ( $\delta TE$ )		
	<i>N</i>	<i>Z</i>	<i>P</i>
<i>N</i>	<i>P</i>	<i>P</i>	<i>Z</i>
<i>Z</i>	<i>P</i>	<i>Z</i>	<i>N</i>
<i>P</i>	<i>Z</i>	<i>N</i>	<i>N</i>

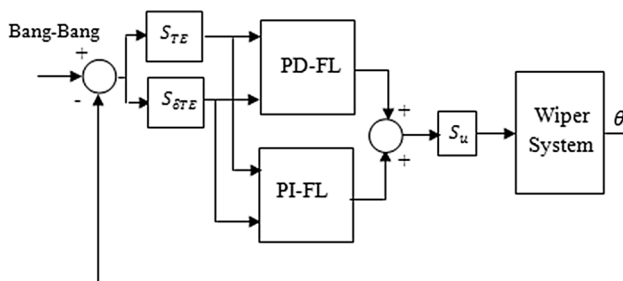


**Fig. 5** PID-FLC

## 3 Results and discussion

### 3.1 Multi-objective indexes

Integral of absolute endpoint acceleration (IAEA), maximum overshoot of hub displacement, and rise time of hub displacement response are objectives that are aimed to be minimized and defined as:

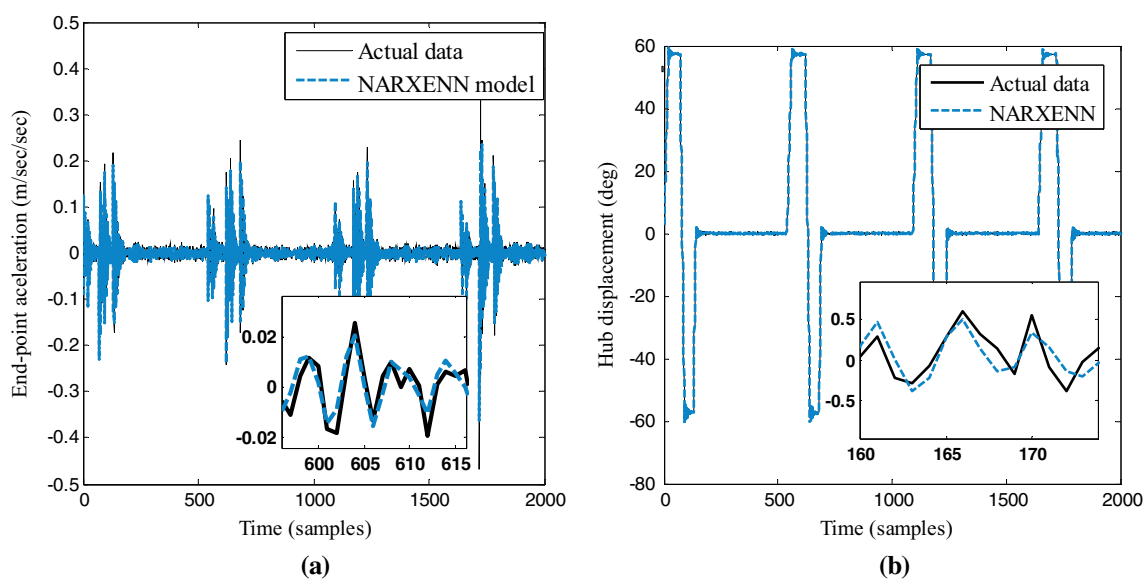


**Fig. 6** Time domain modeling of wiper tip: **a** endpoint acceleration of wiper tip, **b** hub displacement

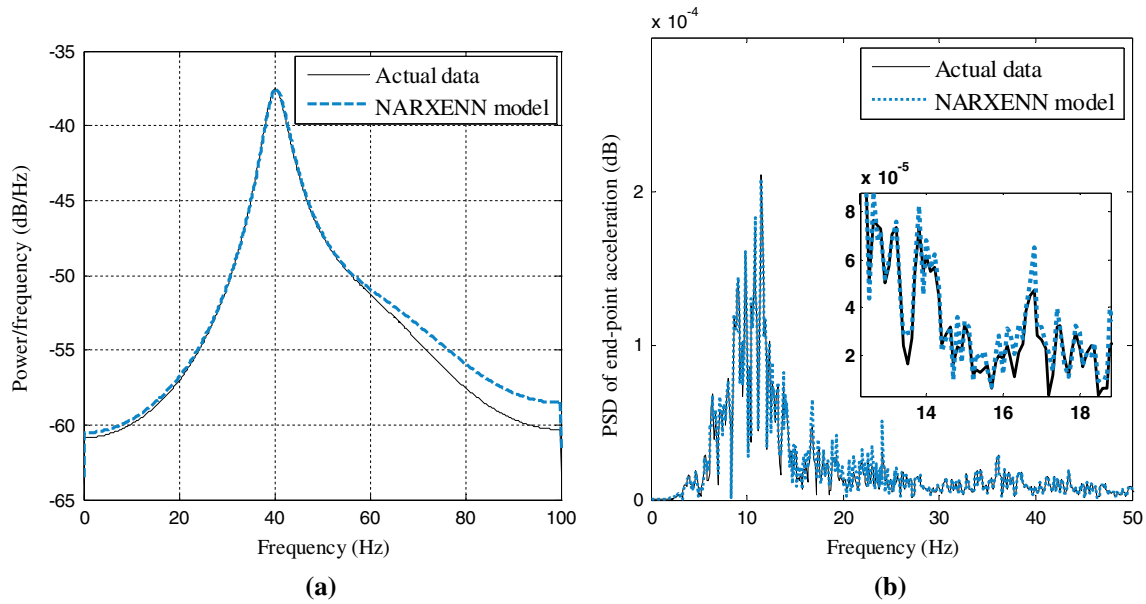


**Fig. 7** Frequency domain modeling of wiper tip response: **a** PSD of endpoint acceleration, **b** Yule-Walker spectral density of endpoint acceleration

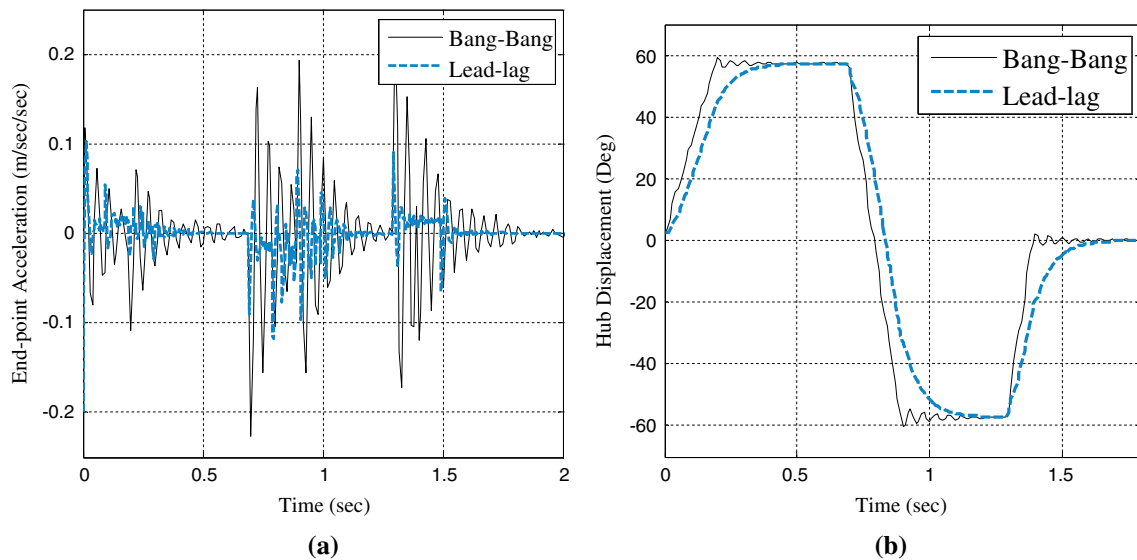


**Fig. 8** Time domain response of wiper tip without disturbance: **a** endpoint acceleration of wiper tip, **b** hub displacement

- Integral absolute value of endpoint acceleration (IAEA):

$$IAEA = \int_0^T |y_{EA}(t)| dt, \tag{5}$$

where  $|y_{EA}(t)|$  represents the vibration amplitude of wiper blade and is correlated to noise level of wiper blade.

- *Rise time* The time required for system hub displacement response to rise from 5 to 95 % of the final steady state value of the desired response.
- *Maximum overshoot* The maximum peak value of the hub displacement response curve measured from the desired response of the system.

In the design of proposed FFL controller, such trade-off is emerged in relationship between rise time and vibration amplitude. IAEA and maximum overshoot are objectives in

accord; while the rise time index of wiper lip is in obvious conflict with two aforementioned objectives.

### 3.2 System identification

As the design of FLC does not require the model of the system, a closed loop system identification procedure is required. A NARXENN is employed to identify a model for the flexible wiper system. The details of the system identification algorithm using the collected experimental data were described in Ref. [33]. For the modeling process, input–output data were collected for a wiper system. Then, performing the one value at the moment the best maximum lag of the data in NARX model was found as  $n_x = n_y = 4$ . Subsequently, ENN with two hidden layers, each with ten tansigmoid neurons and two linear output layers was trained. The process is adjusted until the prediction output satisfied a model validation test and model mean-squared errors level reached to 0.00012. The fitting accuracy of predicted system for one-step-ahead prediction of the corresponding endpoint acceleration and hub angle responses of the actual system is shown in Fig. 6.

It is observed from the NARXENN that the total model order of four is required to model the resonant mode of wiper system. The ultimate goal here is to find a model of the real system that is as simple as possible and yet capable of capturing all of the important characteristics of the plant. The illustrated results of actual and predicted PSD and Yule-Walker power/frequency of endpoint acceleration in frequency domain in Fig. 7 verify that there is an acceptable comparison between system identification results and actual results in frequency domain as well.

### 3.3 Lead–lag controller for single objective

It should be noted that in order to design the conventional controller, the designed lead–lag compensator should be added in series to notch filter to attenuate the effect of structural resonance frequency. The carefully designed lead–lag controller should also be cascaded with a low-pass filter in order to attenuate the high-frequency measurement noise. Figures 8 and 9 show that lead–lag controller is capable of reducing the vibration and noise at the endpoint of the manipulator in comparison with bang–bang input without intervention of any external disturbance.

Further study revealed the deficiency of lead–lag controller in vibration and noise elimination of wiper blade in the presence of external disturbance and uncertainty (Fig. 13). Hence, an essence of a robust controller for reduction in chatter noise level of wiper blade simultaneously with accurate trajectory tracking of wiper hub angle was demanded. In order to achieve such controller, it is required

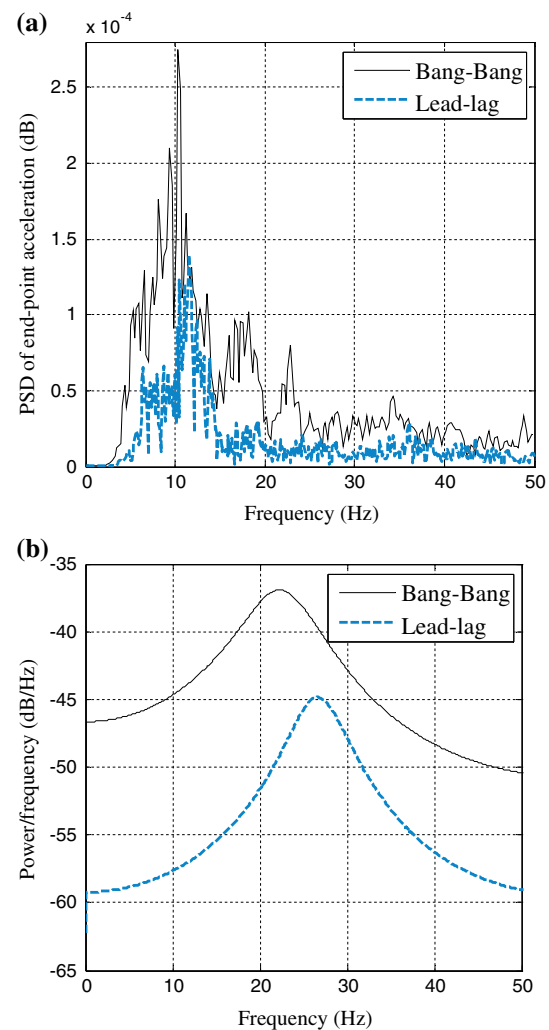


**Fig. 9** Frequency domain response of wiper tip without disturbance: **a** PSD of endpoint acceleration, **b** Yule-Walker spectral density of endpoint acceleration

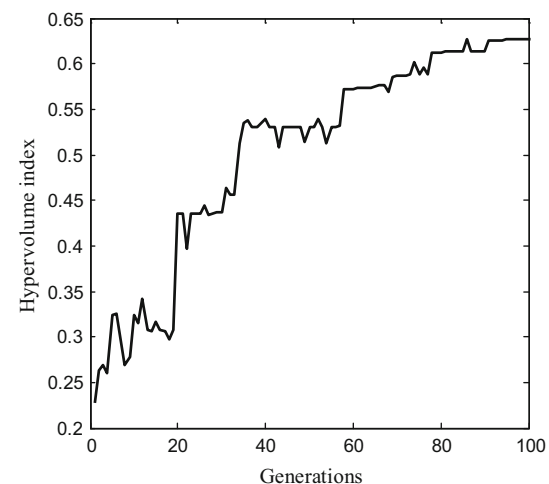


**Fig. 10** Hypervolume indicator of wiper system objective space using MOGA

**Fig. 11** Optimal Pareto sets illustrations of pair objectives: **a** conflict interests, **b** mutual interests

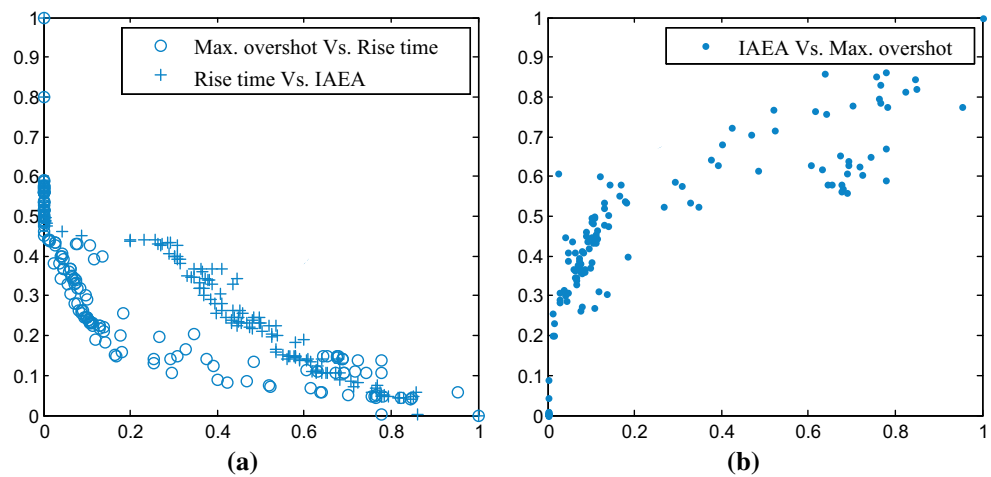


**Table 2** Controller parameters and objective values

Trade no.	Objectives			Controller parameters			
	IAEA (m/s <sup>2</sup> )	Rise time (s)	Max. overshoot (%)	$S_{TE}$	$S_{\delta TE}$	$S_u$	EI
1	924	0.24	93	0.174	0.270	0.023	0.920
2	499	0.32	78	0.235	0.944	0.630	2.134
3	124	0.39	36	0.575	0.376	0.270	1.413
4	468	0.33	51	0.180	0.451	0.445	3.367
5	73	0.48	17	0.411	0.720	0.872	0.892

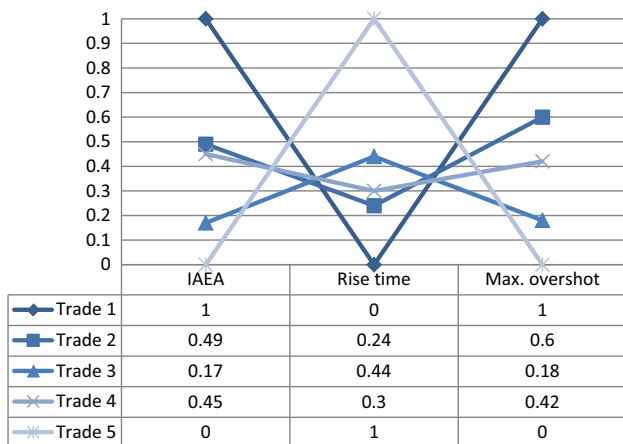


**Fig. 12** Trade-off samples among three-objective Pareto set

to design a robust closed loop controller to reject any unknown external disturbance.

### 3.4 Multi-objective FFL controller

MOGA was initialized with a random population consisting of 50 individuals and maximum generation of 100 as termination criterion. The population is represented by binary strings each of 30 bits, called chromosomes. Each

chromosome consists of five separate strings, constituting three terms specified to PID-FLC membership positions and the rest two specified to proportional and integrative scale factors of IL controller. Using educated guess, a reasonable range of these parameters that ensure stability of system is defined. The crossover rate and mutation rate for this optimization process were set at 90 and 0.01 %, respectively. Moreover, Epanechnikov fitness sharing technique was used to ensure that the best solution of each generation is selected for the next generation, so that the next generation’s best will never degenerate and hence guarantee convergence of the GA optimization process.

Hypervolume indicator assesses the convergence of algorithm toward Pareto front as well as preserving the distribution of Pareto front throughout objectives space. Once this metric is applied to compare the performance of an algorithm in successive iterations; as the number of non-dominated solutions and their distribution throughout the objective space increases, the hypervolume indicator’s value represents the greater value. Hypervolume indicator of MOGA for adjusting controller parameters is shown in Fig. 10. It can be clearly seen that the overall number of Pareto front members found in each generation and their diversity throughout the objective space is increased as the number of generations goes on, so that the maximum value of Hypervolume is obtained at last generation.



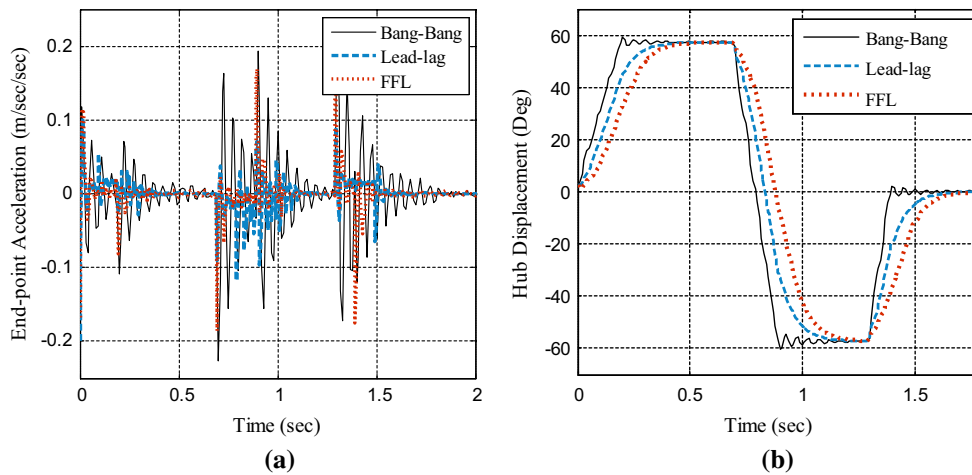


**Fig. 13** Time domain response of wiper tip in the presence of disturbance: **a** endpoint acceleration of wiper tip; **b** hub displacement

Explicit conflict interests of maximum overshoot and IAEA for Pareto optimal sets of wiper blade objectives are illustrated in Fig. 11. This miscorrelation makes the decision tough for designer to choose the best trade-off. However, the non-dominated Pareto set depicted in Fig. 11 proves that IAEA and maximum overshoot are highly non-competing and it is important for the decision-maker, as it conceptually reduces the complexity of the problem.

Adjustable parameters of FFL controller and their corresponding objective measures are listed in Table 2. In Table 2, the most significant non-dominated samples of Pareto optimal sets swinging between the robustness performances and rise time improvement of wiper blade are shown. It can be deduced that the smallest rise time of system is obtained in Trade 2 with unfavorable IAEA and maximum overshoot. Further, the least amounts of vibration objectives are achieved in Trade 5 at the expense of longest rise time. However, in case of current design, the Trade 3 is deemed to be preferred to others that lead to the most reasonable values of IAEA, maximum overshoot, and rise time of wiper blade. Glimpsing at other trade-offs in Table 2 reveals that though Trade 5 has greater vibration reduction and wiper hub trajectory tracking rather than Trade. 3, this is achieved at the expense of longer system delay or rise time. Also, diverse trade-offs of objectives can be seen in Table 2 so that each of them are obtained by adjusting membership functions as well as corresponding scale factors of AFC.

An instance trade-off of Pareto front sets for IAEA, rise time, and maximum overshoot of wiper blade is shown in Fig. 12. The *x*-axis shows the design objectives, and the *y*-axis signifies normalized values of each objective. The conflict interests of objectives are deduced from crossing lines between adjacent objectives, while parallel lines are evident of mutual interests between the objectives.

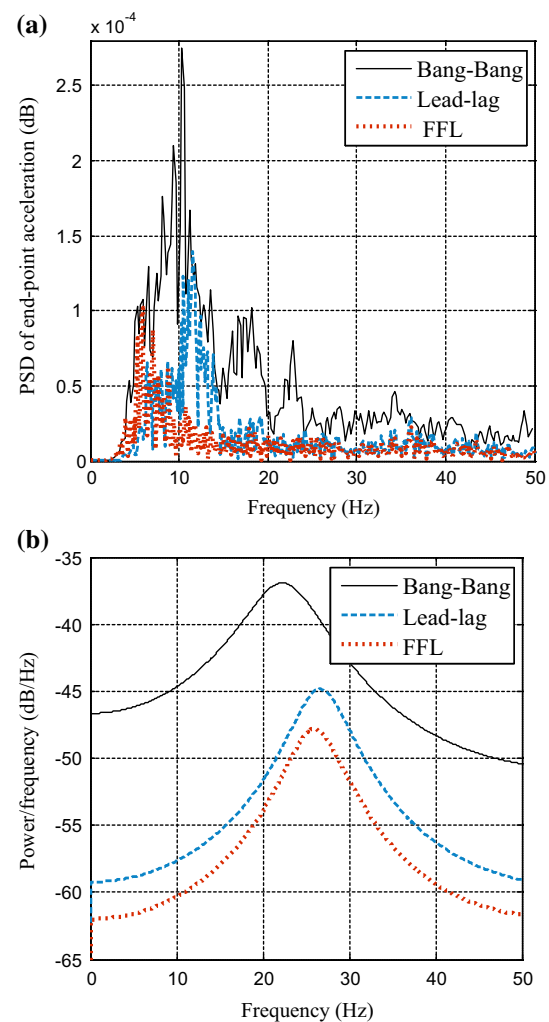


**Fig. 14** Frequency domain response of wiper tip in the presence of disturbance: **a** PSD of endpoint acceleration, **b** Yule-Walker spectral density of endpoint acceleration

As the proposed controller was designed to achieve the greatest vibration and noise reduction in wiper blade in frequency domain while maintaining a reasonable transient response time of system concurrently; convinced the designer to vote on behalf of Trade 3 with the estimated values of IAEA, maximum overshoot, and rise time of wiper blade 178, 27, and 0.26 s, respectively.

The robustness of FFL controller can be obviously deduced from Fig. 13. Figure 13a shows the noteworthy dampening of endpoint acceleration using the FFL controller rather the lead–lag controller with uncertainty. In Fig. 13b, the high distortion of open loop wiper lip in tracking the desired trajectory subjected to external disturbance is evident while the least fluctuation in minimum rise time has been achieved using the FFL controller. Moreover, the deficiency of lead–lag controller in comparison with the proposed controller with applying external disturbance can readily be seen in terms of endpoint acceleration, rise time, and maximum overshoot.

The vibration amplitudes reduction in developed controller is shown in Fig. 14. PSD and Yule-Walker amplitudes of the wiper endpoint that indicate measure of chatter noise of wiper system considerably reduced with FFL controller compared to open loop and IS controller subjected to external disturbance.

#### 4 Conclusion

In dynamics control of flexible manipulators like wiper blade system, usually the low levels of residual vibration cannot be obtained with a command that produces the fastest transient time. In order to achieve the low levels of vibration and noise in frequency domain while maintaining the desirable characteristics of wiper blade in time domain, a lead–lag controller was designed based on the priory knowledge of wiper dynamics system from NARXENN system identification. Conventional lead–lag controller was applied, which reduced vibration and noise of wiper system in a nearly free external disturbance environment. Insensible and deteriorated response of lead–lag controller to uncertainties persuaded the study to devise a more robust controller. Hence, FFL controller was designed by combination of PID-FLC and AFC-based IL. MOGA was employed to settle the most appropriate trade-off among vibration and noise reduction and faster transient time features of wiper system. The results of multi-objective FFL controller were compared with a conventional lead–lag compensator and the bang–bang input in the presence of disturbance. The results showed that the system's performance dramatically improved using FFL compared to the bang–bang input and conventional lead–lag controller. Main contribution of FFL controller than conventional

lead–lag controller is its successful implementation without using any notch filters or low-pass filter while two notch filters and a low-pass filter had to be added to the designed lead–lag compensator before implementing to the system.

#### References

1. Arimoto S, Kawamura S, Miyazaki F (1984) Bettering operation of robots by learning. *J Robot Syst* 1:123–140
2. Ashish S (2013) Vibration suppression of a cart-flexible pole system using a hybrid controller, proceedings of the 1st international and 16th national conference on machines and mechanisms, IIT Roorkee, India, Dec 18–20
3. Awang IM, AbuBakar AR, Ghani BA, Rahman RA, Zain MZM (2009) Complex eigenvalue analysis of windscreen wiper chatter noise and its suppression by structural modifications. *Int J Veh Struct Syst* 1(1–3):24–29
4. Bristow DA, Tharayil M, Alleyne AG (2006) A survey of iterative learning control. *IEEE Control Syst Mag* 26:96–114
5. Chaiyatham T, Ngamroo I (2012) A bee colony optimization based-fuzzy logic-PID control design of electrolyzer for microgrid stabilization. *Int J Innov Comput Inform Control* 8(9):6049–6066
6. Chatterjee A, Pulasinghe K, Watanabe K, Izumi K (2005) A particle swarm optimized fuzzy—neural network for voice-controlled robot systems. *IEEE Trans Ind Electron* 52(6):1478–1489
7. Chen HC (2008) Optimal fuzzy PID controller design of an active magnetic bearing system based on adaptive genetic algorithms, In: the proceedings of international conference on machine learning and cybernetics pp 2054–2060
8. Chen S, Billings SA (1989) Representations of non-linear systems: the NARMAX model. *Int J Control* 49:1013–1032
9. Elman J (1990) Finding structure in time. *J Cognit Sci* 14:179–211
10. Escamilla-Ambrosio PJ, Mort N (2002) A novel design and tuning procedure for PID type fuzzy logic controllers, In: Proceedings of first international IEEE symposium intelligent systems pp 36–41
11. Hewit JR, Burdess JS (1981) Fast dynamic decoupled control for robotics using active force control. *Mech Mach Theory* 16(5):535–542
12. Hung JY (1995) Magnetic bearing control using fuzzy logic. *IEEE Trans Ind Appl* 31:1492–1497
13. Kumar R, Khan M (2007) Pole placement techniques for active vibration control of smart structures: a feasibility study. *J Vib Acoust* 125(5):601–615
14. Li HX, Gatland HB (1996) Conventional fuzzy control and its enhancement. *IEEE Trans Syst Man and Cybern Part B Cyber* 26:791–797
15. Mann GKI, Hu BG, Gosine RG (1999) Analysis of direct action fuzzy PID controller structures. *IEEE Trans Syst Man Cyber Part B Cybern* 29:371–388
16. Noshadi A, Mailah M, Zolfagharian A (2010) Active force control of 3-RRR planar parallel manipulator, *IEEE international conference on mechanical and electrical technology*, Singapore
17. Noshadi A, Mailah M (2012) Active disturbance rejection control of a parallel manipulator with self learning algorithm for a pulsating trajectory tracking task. *Sci Iran* 19(1):132–141
18. Noshadi A, Mailah M, Zolfagharian A (2012) Intelligent active force control of a 3-RRR parallel manipulator incorporating fuzzy resolved acceleration control. *Appl Math Model* 36(6):2370–2383

19. Noshadi A, Shi J, Lee WS, Shi P, Kalam A (2014) Genetic algorithm-based system identification of active magnetic bearing system: a frequency-domain approach. In: Proceedings of international conference of control and automation (ICCA2014), Taiwan, pp 1281–1286
20. Prakash R, Anita R (2012) Modeling and simulation of fuzzy logic controller-based model reference adaptive controller. *Int J Innov Comput Inform Control* 8(4):2533–2550
21. Sahinkaya MN (2001) Input shaping for vibration-free positioning of exible systems. *Proc Instn Mech Eng Part I IMechE* 215:467–481
22. Shaheed MH, Tokhi MO (2002) Dynamic modelling of a single-link of a flexible manipulator: parametric and non-parametric approaches. *J Robot* 20:93–109
23. Silva VVR, Fleming PJ, Sugimoto J, Yokoyama R (2008) Multiobjective optimization using variable complexity modelling for control system design. *Appl Soft Comput* 8:392–401
24. Srinivasan B, Prasad UR, Rao NJ (1994) Backpropagation through adjoints for the identification of non-linear dynamic systems using recurrent neural models. *IEEE Trans Neural Netw* 5(2):213–228
25. Tehrani MG, Mottershead JE, Shenton AT, Ram YM (2011) Robust pole placement in structures by the method of receptances. *Mech Syst Signal Process* 25(1):112–122
26. Tokhi MO, Zain MZM (2006) Hybrid learning control schemes with acceleration feedback of a flexible manipulator system. *Proc Inst Mech Eng Part I J Syst Control Eng* 220(4):257–267
27. Wang Z, Chau KT (2009) Control of chaotic vibration in automotive wiper systems. *Chaos Soliton Fract* 39:168–181
28. Warwick JK, Kang YH, Mitchell RJ (1999) Genetic least squares for system identification. *Soft Comput* 3:200–205
29. Yanyan W, Jiana W, Zhifu Z (2011) Design of intelligent infrared windscreen wiper based on MCU. *Proced Eng* 15:2484–2488
30. Zain MZM, Tokhi MO, Mohamed Z (2006) Hybrid learning control schemes with input shaping of a flexible manipulator system. *Mechatronics* 16:209–219
31. Zhang T, Li HG (2012) Adaptive pole placement control for vibration control of a smart cantilevered beam in thermal environment. *J Vib Control* 18(12):1–11
32. Zitzler E, Thiele L (1999) Multiobjective evolutionary algorithms: a comparative case study and the strength Pareto approach. *IEEE Trans Evol Comput* 3(4):257–271
33. Zolfagharian A, Noshadi A, Khosravani MR, Zain M (2014) Unwanted noise and vibration control using finite element analysis and artificial intelligence. *Appl Math Model* 38:2435–2453